Field observations of wave setup

Steve Lentz and Britt Raubenheimer

Department of Physical Oceanography, Woods Hole Oceanographic Institution, Woods Hole, Massachusetts

Abstract. Wave setup is assumed to be a balance between the cross-shore convergence of the onshore flux of momentum (wave radiation stress S_{xx}) in the surfzone and a cross-shore pressure gradient. Oceanic observations between the 2- and 8-m isobaths near Duck, North Carolina, provide a test of the wave setup balance without assuming that wave height in the surfzone is proportional to water depth. Analysis of data from a cross-shore array of 11 pressure gauges and 10 sonar altimeters deployed during the fall of 1994 indicates the wave setup balance holds to at least the accuracy of the pressure measurements (a few centimeters). The correlation between the two terms in the setup balance is 0.93, and the linear regression slope is 1.05 ± 0.19. Accurate estimates of the cross-shore pressure gradient require density measurements to adjust pressure measurements taken at different depths to the same level. The assumption that pressure and bathymetry are linear between the 2- and 8-m isobaths (or the more common assumption that the height of normally incident, shallow water waves is proportional to the water depth) introduces errors of up to 6 cm for the conditions considered here. Given this assumption, 3.5 years of data from pressure gauges in 2 and 8 m of water indicate that the wave setup balance is valid for a wide range of conditions (correlation 0.71 and regression slope 0.98 ± 0.08).

1. Introduction

Sea level near the coast is set up as surface gravity waves break in shallow water. This wave-driven setup can be substantial (order 1 m) during strong storms [e.g., *Holman*, 1990]. *Longuet-Higgins and Stewart* [1964] hypothesized a dynamical balance between the cross-shore pressure gradient and the momentum flux convergence associated with wave breaking:

$$\rho_o g (\eta + h) \frac{\partial \eta}{\partial x} = -\frac{\partial S_{xx}}{\partial x}, \qquad (1)$$

where η is sea surface elevation, h is water depth, ρ_o is density (assumed to be constant), x and z are the cross-shore and vertical coordinates positive onshore and up, and S_{xx} is the onshore component of the wave-driven momentum flux tensor or wave radiation stress. (In (1) and what follows all quantities are averages over timescales long compared with surface gravity wave periods.)

Longuet-Higgins and Stewart [1962] showed the wave radiation stress from linear wave theory is, to second-order,

$$S_{xx} = E \left\{ [\cos^2 (\theta) + 1] \frac{C_g}{C} - \frac{1}{2} \right\}, \qquad (2)$$

where $E = \rho_o g H^2 / 8$ is wave energy, g is gravitational acceleration, H is wave height, C_g and C are the group velocity and phase speed, and θ is the wave direction. Although linear wave theory to second order should not be valid in the surfzone [e.g., *Bowen et al.*, 1968; *Svendsen*, 1984], previous results suggest that local estimates are reasonably accurate [*Guza and Thornton*, 1980, 1981].

Bowen et al. [1968] noted that (1) could be simplified by assuming normally incident, shallow water waves so (2) re-

duces to $S_{xx} = 1.5E$ and assuming wave height within the surfzone is limited by the mean water depth:

$$H = \gamma (\eta + h), \qquad (3)$$

where γ is an empirical constant. These two assumptions imply that sea surface slope is proportional to bottom slope,

$$\frac{\partial \eta}{\partial x} = -\frac{3\gamma^2/8}{1 + 3\gamma^2/8} \frac{\partial h}{\partial x}, \qquad (4)$$

and setup at the shoreline η_c is proportional to the wave height H_b at the offshore edge of the surfzone

$$\eta_c = \frac{3}{8} \gamma H_b. \qquad (5)$$

Laboratory studies have shown close agreement between the terms in (1), (4), or (5) [e.g., *Bowen et al.*, 1968; *Battjes*, 1974; *Battjes and Stive*, 1985] offshore of the shallow water on the beachface (runup) where the setup gradient is larger than predicted. Other theoretical and laboratory studies have suggested wave roller processes must be included to describe accurately the radiation stress of shallow water waves and the resulting wave setup [*Svendsen*, 1984; *Diegaard et al.*, 1991; *Schäffer et al.*, 1993].

As noted by *Holman* [1990], explicit tests of (1) using oceanic observations are lacking. Field studies focused on (5) have shown an approximately linear relationship between shoreline setup and wave height with $0.6 \leq \gamma \leq 1.3$ estimated from linear regression analyses [*Guza and Thornton*, 1981; *Holman and Sallenger*, 1985; *Nielsen*, 1988]. (For the field observations, γ corresponds to the root-mean-square (rms) wave heights H_{rms}, defined as $2\sqrt{2}\sigma$, where σ is the standard deviation of the sea surface fluctuations.) Although these values of γ are consistent with those estimated from (3) for laboratory observations of monochromatic waves [*Bowen et al.*, 1968; *Battjes*, 1974; *Battjes and Stive*, 1985], comparisons of surfzone field observations with (3) have typically shown $0.2 \leq \gamma \leq 0.5$ [*Sallenger and*

Holman, 1985; *Raubenheimer et al.*, 1996], much lower than that needed to satisfy (5). Assuming a constant beach slope, *Nielsen* [1988] and *King et al.* [1990] showed rough agreement between surfzone setup observations and (4) with $\gamma = 0.5$ and 0.35, respectively. However, the field observations generally exhibit large (~100%) scatter relative to (4) and (5) that has been attributed to inaccuracies in the setup balance ((1) and (2)) at the beachface and inaccuracies in (3). Because of the dependence of γ on wave characteristics and bottom slope [*Bowen et al.*, 1968; *Sallenger and Holman*, 1985; *Raubenheimer et al.*, 1996], it has been unclear whether errors in the wave setup balance would increase for a larger range of conditions.

The large scatter in comparisons of (4) and (5) with field observations may also be because of the terms in the cross-shore momentum balance neglected in deriving (1). *Lentz et al.* [1999] estimated the cross-shore acceleration, the Coriolis force due to the alongshore flow, the cross-shore wind stress, and the cross-shore bottom stress using current measurements from a tower spanning the water column at the 4-m isobath and wind measurements from the Field Research Facility (FRF) pier acquired August–October 1994. These four terms were at least an order of magnitude smaller than estimates of $\partial S_{xx}/\partial x$ at the 4-m site and estimates presented here, supporting the assumption that (1) is the dominant balance in the near shore. However, the order of magnitude of the bottom stress is uncertain, and the nonlinear advective terms associated, for example, with alongshore bathymetric features and infragravity waves, were not estimated and may be large.

Pressure, sonar altimeter, and density observations acquired in 2–8-m water depth offshore of the Army Corps of Engineer's FRF near Duck, North Carolina, during the fall of 1994 are used to examine the balance of terms in (1) using (2) to estimate S_{xx}, but without assuming (3), so there are no free parameters. The comparison focuses on the surfzone (2–8 m), avoiding the shallow water of the beachface where (1) is known not to be valid [*Bowen et al.*, 1968; *Nielsen*, 1988]. Data acquired between 1993 and 1998 from a pair of pressure gauges are used to test (1) and (2) over a much longer period than previous studies and hence a wider range of conditions. One result of the present study is that alongshore bathymetric variations, infragravity waves, wind, and other complications of the natural environment do not substantially degrade the comparisons of the theory with field data relative to comparisons with measurements in narrow laboratory flumes.

2. Methods

2.1. Fall 1994 Data

An array of 10 pressure sensors and sonar altimeters (to measure the seafloor location) colocated in water depths of 2–5 m and a single pressure sensor located in 8-m water depth were deployed along a transect perpendicular to the shoreline ~400 m northwest of the FRF pier as part of the Duck94 study (Figure 1). Data were collected nearly continuously from mid-August to mid-October 1994 at a 2-Hz sampling rate. Bathymetric changes were significant during the experiment, with up to 1.5-m erosion and 1-m accretion along the transect [*Gallagher et al.*, 1998], and sensors were raised or lowered to maintain an elevation above the sand bed of ~0.4–1.0 m. A continuous time series of density is available from a SeaBird Seacat mounted on the FRF pier as part of the Coastal Ocean Processes Inner Shelf Study field program [*Butman*, 1994]. The
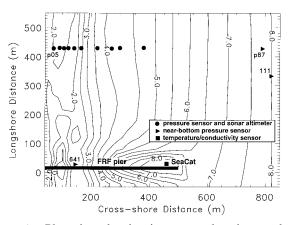

Figure 1. Plan view showing instrument locations and bathymetry on September 20, 1994.

Seacat was located 4 m above the seafloor in 8 m of water and took a sample every 4 min.
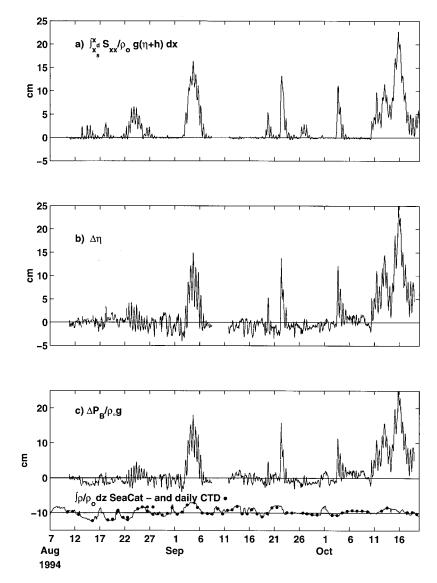
Pressure and sonar altimeter data were corrected for temperature and changes in sensor elevation. Mean pressure P_B and seafloor location were recorded for each 3-hour long data run. Using pressure and altimeter data, times when the shallowest pressure sensors may have come out of the water were flagged and not considered in subsequent analysis. $H_{\mathrm{rms}} = 2\sqrt{2}\sigma$ was calculated for the sea swell frequency band ($0.04 \le f \le 0.30$ Hz) using a linear theory depth correction. Processing of the Seacat data was straightforward and is documented by *Alessi et al.* [1996]. The fall 1994 data were averaged and interpolated to hourly values to facilitate comparisons.

2.2. FRF Data

A much longer time series is available from a pair of near-bottom pressure sensors deployed and maintained by personnel at the Army Corps of Engineers FRF. Pressure gauge 641 is located ~150 m offshore and 0.4 m above the seafloor in 2 m of water on the FRF pier (Figure 1). The FRF pier alters the local bathymetry [*Miller et al.*, 1983], which may influence the pressure field. Pressure gauge 111 is ~800 m offshore and ~300 m northwest (alongshore) of the FRF pier at a depth of 7.8 m. Pressure gauge 111 is the central element in a 15-element wave directional pressure array maintained by the FRF. Gauge 641 has been in service since November 1992, and gauge 111 has been in service since September 1986, though there are data gaps in each time series. Part of a large data gap (August 1995 to July 1996) for gauge 111 was filled with data from gauges 121 (February 1996) and 131 (March to June 1996) that are also part of the wave directional array. Additionally, daily conductivity-temperature-depth (CTD) profiles have been taken at the end of the pier since 1994.

Data from both pressure gauges are processed at the FRF, and mean pressure, significant wave height, and peak wave period T_p, over 34-min records are reported [*Long*, 1996]. The peak wave period is the period associated with maximum energy in the spectrum. The wave direction θ associated with the energy spectral peak at the 8-m site is estimated from the wave directional array data using an iterative maximum likelihood estimator [*Pawka*, 1983].

Additional processing of the FRF pressure data was required. The bottom pressure data were first truncated to focus on two time periods, October 11, 1993, to August 15, 1995, and

Figure 2. Time series of terms in (8) and (9) for the fall 1994 period August 4 to October 20. (c) The density term has been shifted −10 cm for clarity.

February 1, 1996, to March 10, 1998, when both gauges were working and pressure differences did not have large shifts (5 cm or more) on short timescales (days to weeks). (Pressures are reported in centimeters of water, which are roughly equivalent to millibars.) Offsets of 3–65 cm were subjectively removed so that the average pressure difference in the absence of large waves was approximately zero. The offsets are probably due to differences in the gauge depths when instruments were serviced and redeployed. Two drifts (20 cm over 130 days and 6 cm over 60 days) and a "seasonal" variation with an amplitude of ~10 cm (mid-November 1996 to mid-May 1997) were also removed. The latter may have been due to the uncorrected temperature dependence of the pressure sensors and is consistent with 1°C, causing an apparent 0.5-cm pressure difference. See *Wearn and Larson* [1982] for discussion of pressure sensor drifts and temperature dependence. To minimize a consistent relative gain error between the two FRF pressure gauges of ~3.5%, the bottom pressure time series for the 2-m site was multiplied by 1.035. This correction had little

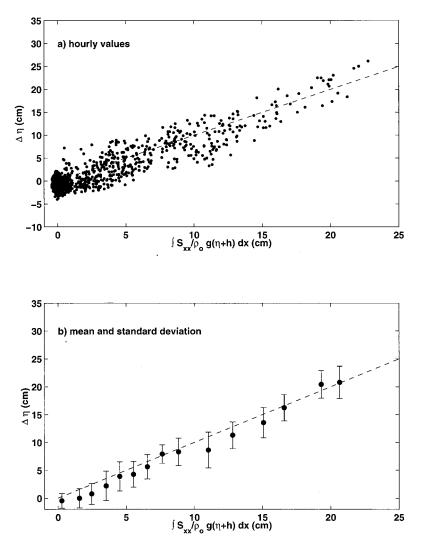effect on the inferred setup, aside from reducing the tidal variations.

2.3. Estimation of Terms

If density is not constant (as assumed in (1)) and if the flow is hydrostatic for timescales of hours and longer, the pressure $P(z)$ may be expressed as

$$P(z) = \rho_o g \eta + \int_z^0 \rho g \, dz, \qquad (6)$$

where $g = 9.8$ m s^{-2} is gravitational acceleration, $\rho_o = 1023$ kg m^3 is a reference density, and $z = 0$ is a fixed reference level just below the sea surface. The depth-integrated cross-shore pressure gradient then is given by

$$\int_{-h}^{\eta} \frac{\partial P}{\partial x} \, dz = \rho_o g \, \frac{\partial \eta}{\partial x} \, (\eta + h) + \int_{-h}^{\eta} \int_z^0 g \, \frac{\partial \rho}{\partial x} \, dz' \, dz.$$

$$(7)$$

Figure 3. $\Delta\eta$ versus $\int(\partial S_{xx}/\partial x)/\rho_o g(\eta + h)\ dx$: (a) scatter plot of hourly values and (b) means and ± 1 standard deviation of binned data. In Figures 3a and 3b the dashed line has a slope of 1. Linear regression slope and correlation are listed in the first row of Table 1.

Density measurements were only available near the end of the pier, so time series of the cross-shore density gradient are not available. Rough estimates of the cross-shore density gradient term in (7) between the 2- and 8-m isobaths from small boat

Table 1. Results of Linear Regression Between Terms in (8) or (10) of the Form $\Delta\eta = aF + b$ for 62 Days in Fall 1994

| | Standard Deviations | | | |
| | --- | --- | | |
F	F	$\Delta\eta$	Slope	Correlation
$\int(\partial S_{xx}/\partial x)/\rho_o(\eta + h)\ dx$	4.1	4.6	1.05 ± 0.19	0.93
$\Delta S_{xx}/\rho_o gh_{avg}\ h_{avg}$ from (11)*	4.3	6.0	1.25 ± 0.64	0.91
$\Delta S_{xx}/\rho_o gh_{avg}$	2.8	4.6	1.48 ± 0.27	0.91
$h_{avg} = (h_s + h_d)/2$				

Correlations are significantly different from zero at the 95% confidence level, and the 95% confidence intervals for regression slopes are listed on the basis of an estimated independence timescale of 3 days. Units are in centimeters.

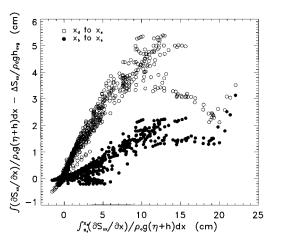*Regression using (8) includes only 20 days of data when surfzone was estimated to be seaward of shallow site.

surveys taken from August to October 1994 [*Largier and Millikan*, 1996] suggest that this term was about an order of magnitude smaller than the barotropic pressure gradient (first term on right-hand side of (7)) and is probably negligible in the surfzone in most circumstances. Substituting (7) into (1), neglecting the cross-shore density gradient, dividing by $\rho_o g(\eta + h)$, and integrating cross-shore from the deep (x_d) to the shallow (x_s) pressure gauge site yields

$$\Delta\eta = -\int_{x_d}^{x_s} \frac{1}{\rho_o g(\eta + h)} \frac{\partial S_{xx}}{\partial x}\ dx, \tag{8}$$

where $\Delta\eta$ is the sea level difference between x_s and x_d. Using (6) and assuming cross-shore density gradients are small, as noted above, $\Delta\eta$ may be estimated from density and near-bottom pressure observations:

$$\Delta\eta = \frac{\Delta P_B}{\rho_o g} - \int_{h_d}^{h_s} \frac{\rho}{\rho_o}\ dz|_{x_d}, \tag{9}$$

where h_s and h_d are the water depths at the shallow and deep sites. The second term on the right-hand side of (9) is a density

Figure 4. Shown is $\int (\partial S_{xx}/\partial x)/\rho_o g(\eta + h)\, dx - \Delta S_{xx}/\rho_o g h_{avg}$ versus $\int_{x_s}^{x_d} (\partial S_{xx}/\partial x)/\rho_o g(\eta + h)\, dx$ for the fall 1994. Here $\int (\partial S_{xx}/\partial x)/\rho_o g(\eta + h)\, dx - \Delta S_{xx}/\rho_o g h_{avg}$ is evaluated between x_d and x_s (open circles) and between x_b and x_s (solid circles).

correction required to bring the bottom pressures to the same level. Without this correction, temporal variations in density, which result in bottom pressure difference fluctuations, may be misinterpreted as cross-shore pressure gradients.

Estimation of the terms in (8) is straightforward using the fall 1994 pressure and sonar altimeter data and the Seacat data from the FRF pier. $\Delta\eta$ is estimated from (9) using the pressure difference between p05 and p87 (Figure 1) and the pier Seacat data assuming density is vertically uniform. Comparison of estimates from the daily CTD profiles with estimates from the single-pier Seacat (Figure 2c) indicates that vertical structure does not have a large effect on the density correction in (9). Wave radiation stresses are estimated at each site following (2) with $E = \rho_o g H_{rms}^2/8$ and C_g and C estimated using the dispersion relationship, the total water depth ($\eta + h$), and the peak wave period T_p. Wave direction θ is estimated from the 8-m wave direction, Snell's law, and C at each site. Wave direction estimates based on a directional moment technique [*Elgar et al.*, 1994; *Herbers and Guza*, 1990] rather than the peak wave direction reported by the FRF yield very similar estimates for S_{xx} for fall 1994. At the 8-m FRF site, S_{xx} estimated using the directional moment technique, sea swell energy, and directional spectra is well correlated (correlation 0.995) with S_{xx} estimated from bulk properties (H_{rms}, θ, C_g, and C); however, the magnitudes differ by up to ~30%. Errors associated with using the bulk quantities may contribute to the scatter in the results. Water depth h is calculated using the tidal elevation estimated at p87 and the observed seafloor location at each sensor. The integral on the right-hand side of (8) is evaluated using a fourth-order Runga-Kutta scheme with a horizontal step size of 0.1 m. Setup contributes to the denominator on the right-hand side of (8). Therefore the integral is estimated iteratively by initially assuming that η at each horizontal step is equal to that calculated at the previous step, determining $\eta(x)$, and then recomputing the integral.

For the FRF data the cross-shore structure of η, h, and $\partial S_{xx}/\partial x$ are not known. However, assuming η is linear between the shallow and deep sites and integrating (1) from x_d to x_s yields

$$\Delta\eta = \frac{\Delta S_{xx}}{\rho_o g h_{avg}}, \qquad (10)$$

where

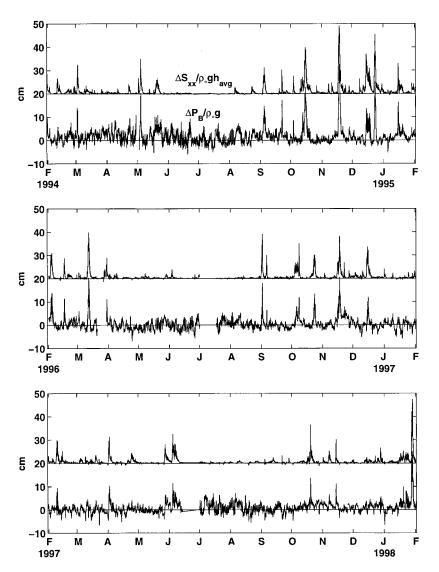$$\frac{1}{(x_d - x_s)} \int_{x_s}^{x_d} (\eta + h)\, dx = h_{avg} \approx \frac{[(\eta_s + h_s) + (\eta_d + h_d)]}{2}$$

and h is also assumed to be linear to estimate h_{avg}. (Equation (10) also follows from assuming normally incident, shallow water waves, and depth-limited wave height (3). However, in contrast to (4) and (5), (10) is independent of γ and therefore is less restrictive. Furthermore, the variation of γ with wave conditions and beach slope does not result in errors.) The water depth is calculated using the observed pressure and assuming a constant seafloor location. The density correction in (9) estimated from the daily pier CTD casts from August 1994 through March 1998 has a standard deviation of 1.3 cm and a range of ±3 cm. However, this density correction is not included in the FRF estimates of $\Delta\eta$ because uncertainties in the FRF pressure data are about twice the density correction, the intermittent daily CTD casts often do not resolve the dominant temporal variability (Figure 2c), and CTD casts were often not taken during big wave events. The pressure and wave radiation stress differences in (10) are estimated from the two FRF pressure sensors using the procedure described above. The validity of assuming η and h are linear is examined in section 3 using the fall 1994 data.

2.4. Data Uncertainties

Problems cited in sections 2.1 and 2.2 indicate bottom pressure differences have uncertainties of several centimeters or more because of inaccurate removal of offsets, drifts, and the uncorrected temperature dependence of the FRF gauges. Additionally, there are errors due to adjustment of the flow around the instrument case resulting in pressure variations at the sensor port (flow noise). Using Bernoulli's equation, flow noise is proportional to the square of the flow speed. For a velocity of 1 m s^{-1} due to waves and mean flow, with the worst case scenario of the pressure port facing into the maximum flow, the error is 5 cm in pressure. Comparisons of terms estimated using FRF gauges 111 and 641 with those estimated from p87 and p05 for the overlapping fall 1994 time period indicate rms differences of 2.5 cm (range ±5 cm) for $\Delta P_B/\rho_o g$ and 0.5 cm (range ±2 cm) for $\Delta S_{xx}/\rho_o g h_{avg}$. The differences appear to be primarily associated with offsets and the uncorrected temperature response of the FRF gauges. The differences are independent of H_{rms}, suggesting that flow noise either is not large or has a tendency to cancel. The agreement between the pressure differences 111 minus 641 and p87 minus p05 during set-up events (differences of a few centimeters) indicate that the complex bathymetry associated with the FRF pier (Figure 1) does not have a large influence on the setup between the 8- and 2-m isobaths.

3. Results

The time series of the two terms in (8) for the fall 1994 period (Figures 2a and 2b), mid-August to mid-October, are well correlated with a linear regression slope of ~1.0 (Figure 3 and Table 1). The time series are dominated by a few events when waves are large ($H_{rms} > 0.7$ m), lasting 1–10 days. The largest event (October 15) had a peak rms wave height of 3 m
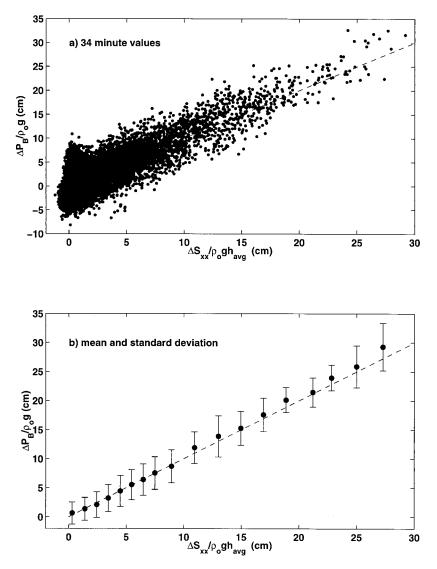
Figure 5. Time series of $\Delta P_B/\rho_o g$ and $\Delta S_{xx}/\rho_o g h_{\mathrm{avg}}$ from February to January for 1994, 1996, and 1997. $\Delta S_{xx}/\rho_o g h_{\mathrm{avg}}$ time series are shifted +20 cm for clarity.

and a peak setup between p87 and p05 of 25 cm. The rms difference between the two terms in (8) is 1.8 cm, which is well within the uncertainty of the pressure measurements. Examination of the time series suggests that some of the discrepancy is associated with offsets of a couple centimeters (middle to late September) in $\Delta\eta$. Thus, for these observations the wave radiation stress convergence and the cross-shore pressure gradient balance to the accuracy of the measurements (Figures 2a and 2b).

The density corrections in (9) are small compared with the wave-driven set-up events in bottom pressure difference (Figure 2c). The density correction has a standard deviation of 1 cm and a range of ± 2 cm, compared with a standard deviation of 4.5 cm for the bottom pressure difference with peak values over 20 cm. Nevertheless, there is a correspondence between $\Delta P_B/\rho_o g$ and the density correction during periods of small waves, for example, mid-August and mid-September. Fluctuations in the density term are primarily due to density variations of up to 5 kg m^{-3} ($\approx 0.5\%$) associated with the Chesapeake Bay plume [*Rennie et al.*, 1999]. If uncorrected, these temporal density variations will result in errors in estimates of sea level

difference of 0.5% of the water depth that could be misinterpreted as setup or setdown.

The accuracy of (10) relative to (8) is examined with the fall 1994 data. $\Delta S_{xx}/\rho_o g h_{\mathrm{avg}}$ underestimates the right-hand side of (8) (Figure 4). The difference between the two estimates increases as a function of $\int_{x_s}^{x_d} 1/\rho_o g(\eta + h)\ \partial S_{xx}/\partial x\ dx$, reaching a maximum of ~ 6 cm for moderate wave heights and then decreasing for larger wave heights. A major part of the discrepancy is due to the offshore edge of the surfzone, x_b, being onshore of the deep site, so there is a region of shoaling waves where there is setdown rather than setup (e.g., η is not linear) and waves are not limited by water depth (e.g., (3) is not valid). (A rough estimate assuming shallow water waves indicates that the setdown is <1 cm.) When (8) and (10) are evaluated between x_b and x_s, where x_b is the offshore edge of the surfzone, assumed to be where $h = H_{\mathrm{rms}}/\gamma$ with $\gamma = 0.33$, the maximum discrepancy is reduced to ~ 3 cm (Figure 4). Estimating (10) between x_b and x_s using the bathymetry from all the sonar altimeters to evaluate h_{avg} reduces the discrepancy by about half. The remaining discrepancy is presumably due to assuming η is linear within the surfzone.

Figure 6. $\Delta P_B/\rho_o g$ versus $\Delta S_{xx}/\rho_o gh_{\mathrm{avg}}$: (a) scatterplot of 34-min values and (b) means and ± 1 standard deviation of binned data. In Figures 6a and 6b the dashed line has a slope of 1. Linear regression slope and correlation are listed in the first row of Table 2.

For the longer FRF data set, which contains observations at only two locations, (10) can be partially corrected by estimating the average surfzone water depth between x_s and the minimum of x_b and x_d as

$$h_{\mathrm{avg}} = (h_s + h_o)/2 \qquad h_o = \min (H_{111}/\gamma, h_d), \qquad (11)$$

where H_{111} is the rms wave height at sensor 111 and only times when h_o is greater than h_s are considered. For the fall data, using $\gamma = 0.33$, this modification reduces the peak discrepancy between (8) and (10) by ~40% (not shown). The correlation between the two terms in (10) with $h_{\mathrm{avg}} = (h_s + h_d)/2$ or using (11) is about the same as for the two terms in (8) (Table 1). However, the regression slopes are >1 because $\Delta S_{xx}/\rho_o gh_{\mathrm{avg}}$ underestimates the right-hand side of (8).

The time series of the terms in (10) from the FRF data (Figure 5) exhibit the same correspondence seen in Figure 2. For the complete 43 months of data, there were ~30 events with setups >10 cm between the deep and shallow sensors (corresponding roughly to rms wave heights >2 m). Large

events primarily occur during fall and winter and are rare during summer. The largest observed setup was over 30 cm during Hurricane Gordon in mid-November 1994.

$\Delta S_{xx}/\rho_o gh_{\mathrm{avg}}$ and $\Delta P_B/\rho_o g$ exhibit a linear relationship and are well correlated (Figure 6 and Table 2). Thus this extensive data set provides compelling support for (1) and (2) over a

Table 2. Results of Linear Regression Between Terms in (10) of the Form $\Delta P_B/\rho_o g = a(\Delta S_{xx}/\rho_o gh_{\mathrm{avg}}) + b$

Data	Slope	Correlation	Days
all data	0.98 ± 0.08	0.71	1314
$H_{111}/\gamma > h_s$	1.06 ± 0.09	0.84	449
h_{avg} from (11)	0.90 ± 0.08	0.83	449

Correlations are all significantly different from zero at the 99% confidence level, and the 95% confidence intervals for regression slopes are listed on the basis of an estimated independence timescale of 3 days. Units are in centimeters.

wide range of conditions. A large fraction of the time waves are small enough that the surfzone is probably onshore of gauge 641. If only events with $H_{111}/\gamma > h_s$ are considered, the correlation increases, and the regression slope remains ~1.0. Use of (11) to estimate h_{avg}, which only considers $H_{111}/\gamma > h_s$, does not improve the comparison (Table 2). In either case, rms differences between the two terms are 2.5 cm, only slightly larger than for the more complete fall 1994 observations (1.8 cm) and within the accuracy of the pressure measurements. Other factors contributing to the scatter are the assumption that η and h are linear, i.e., using (10) rather than (8); the use of bulk properties and second-order linear theory (2) to estimate S_{xx}, the uncertainties in the seafloor location and water depth, and the failure to include the density correction in (9).

4. Summary

Two sets of oceanic observations acquired near Duck, North Carolina, provide field tests of the wave setup balance (1) [*Longuet-Higgins and Stewart*, 1964] between the wave radiation stress convergence estimated from linear wave theory (2) and the cross-shore pressure gradient. In contrast to previous studies, the wave set-up balance was tested without considering the region of runup on the beachface where (1) is known not to be valid [*Bowen et al.*, 1968; *Nielsen*, 1988] and without assuming that wave height in the surfzone is proportional to the mean water depth (3) [*Bowen et al.*, 1968]. By avoiding use of the free parameter γ, which depends on wave characteristics and bottom slope [*Raubenheimer et al.*, 1996] and hence can vary from site to site and from one set-up event to the next, the accuracy of (1) and (2) can be tested less ambiguously. The major limitation in this study was the accuracy of the pressure measurements due to uncertainty in offsets and gains, flow noise, and uncorrected temperature dependence (FRF instruments).

Observations from a cross-shore array of 11 pressure gauges and 10 sonar altimeters spanning the surfzone (2–8-m isobaths) deployed for 2 months during the fall of 1994 allow a straightforward integration of (1). The results indicate that (1) is valid to the accuracy of the pressure measurements (a few centimeters) (Figures 2 and 3). Assuming that both the pressure and water depth vary linearly across the surfzone (so that (1) simplifies to (10)), measurements from a pair of pressure gauges in 2 and 8 m of water maintained by the FRF spanning 3.5 years show that the wave set-up balance holds to the accuracy of the measurements over a wide range of wave conditions (Figures 5 and 6). The close agreement between the setup observations and the theories also implies that (2) is an accurate representation of S_{xx} in the surfzone.

The extensive pressure and sonar altimeter array in fall 1994 allowed a direct estimate of the errors owing to the simplified set-up balance (equation (10)). Assuming that both the pressure and bathymetry were linear between the 2- and 8-m isobaths introduced errors in the estimated setup of up to 6 cm during fall 1994 (Figure 4). Three factors contributed to this error: the offshore edge of the surfzone being onshore of the 8-m site, curvature in the bottom bathymetry, and curvature in the pressure within the surfzone. Thus the cross-shore structure of both the bathymetry and the pressure or the wave radiation stress is required for accurate tests of (1).

In regions where density variations in the near shore are large, for example, near rivers or estuaries [*Hanslow et al.*, 1997], accurate pressure gradient estimates require density

measurements to adjust pressure measurements from sensors at different depths to the same level (equation (9)). The Duck site is ~100 km from the mouth of Chesapeake Bay, the source of the density variability [*Rennie et al.*, 1999], indicating that density variations associated with freshwater plumes can be important even relatively far from the source.

Wave-driven setup between the 2- and 8-m isobaths often exceeded 10 cm at Duck, North Carolina (Figures 2 and 5). These large wave setups suggest that caution is required in using tide gauges or shallow pressure gauges to estimate larger-scale cross-shore or alongshore pressure gradients [e.g., *Lentz and Winant*, 1986]. Two sensors in slightly different water depths could yield apparently large gradients during moderate to large waves because of wave setup.

References

Alessi, C. A., S. J. Lentz, and J. Austin, Coastal Ocean Processes Inner-Shelf Study: Coastal and moored physical oceanographic measurements, *Tech. Rep. WHOI-96-06*, 142 pp., Woods Hole Oceanogr. Inst., Woods Hole, Mass., 1996.

Battjes, J. A., Computations of set-up, longshore currents, run-up overtopping due to wind-generated waves, *Tech. Rep. 74-2*, Delft Univ. of Technol., Delft, Netherlands, 1974.

Battjes, J. A., and M. J. F. Stive, Calibration and verification of a dissipation model for random breaking waves, *J. Geophys. Res.*, *90*, 9159–9167, 1985.

Bowen, A. J., D. L. Inman, and V. P. Simmons, Wave "set-down" and set-up, *J. Geophys. Res.*, *73*, 2569–2577, 1968.

Butman, C. A., CoOP: Coastal Ocean Processes Study—Interdisciplinary approach, new technology to determine coupled biological, physical, geological processes affecting larval transport on inner shelf, *Sea Technol.*, *35*, 44–49, 1994.

Diegaard, R., P. Justesen, and J. Fredsøe, Modeling of undertow by a one-equation turbulence model, *Coastal Eng.*, *15*, 431–458, 1991.

Elgar, S., T. H. C. Herbers, and R. T. Guza, Reflection of ocean surface gravity waves from a natural beach, *J. Phys. Oceanogr.*, *24*, 1503–1511, 1994.

Gallagher, E. L., S. Elgar, and R. T. Guza, Observations of sand bar evolution on a natural beach, *J. Geophys. Res.*, *103*, 3203–3215, 1998.

Guza, R. T., and E. B. Thornton, Local and shoaled comparisons of sea surface elevations, pressures, and velocities, *J. Geophys. Res.*, *85*, 1524–1530, 1980.

Guza, R. T., and E. B. Thornton, Wave set-up on a natural beach, *J. Geophys. Res.*, *86*, 4133–4137, 1981.

Hanslow, D. J., P. Nielsen, and K. Hibbert, Wave setup at river entrances, paper presented at 25th International Conference on Coastal Engineering, Am. Soc. of Civ. Eng., Orlando, Fla., 1997.

Herbers, T. H. C., and R. T. Guza, Estimation of directional wave spectra from multicomponent observations, *J. Phys. Oceanogr.*, *20*, 1703–1724, 1990.

Holman, R. A., Wave set-up, in *Handbook of Coastal and Ocean Engineering Wave Phenomena and Coastal Structures*, edited by J. B. Herbich, pp. 635–646, Gulf, Houston, Tex., 1990.

Holman, R. A., and A. H. Sallenger Jr., Setup and swash on a natural beach, *J. Geophys. Res.*, *90*, 945–953, 1985.

King, B. A., M. W. L. Blackley, A. P. Carr, and P. J. Hardcastle,

Observations of wave-induced set-up on a natural beach, *J. Geophys. Res.*, *95*, 22,289–22,297, 1990.

Largier, J. L., and K. S. Millikan, Coastal Ocean Processes (CoOP) pilot project data report: August–October 1994 R/V *Moby Duck* CTD and underway data, *Tech. Rep. SIO Ref. Ser. 96-29*, 240 pp., Scripps Inst. of Oceanogr., La Jolla, Calif., 1996.

Lentz, S. J., and C. D. Winant, Subinertial currents on the southern California shelf, *J. Phys. Oceanogr.*, *16*, 1737–1750, 1986.

Lentz, S. J., R. T. Guza, S. Elgar, F. Feddersen, and T. H. C. Herbers, Momentum balances on the North Carolina inner shelf, *J. Geophys. Res.*, *104*, 18,205–18,226, 1999.

Long, C. E., Index and bulk parameters for frequency-distribution spectra measured at CERC Field Research Facility, June 1994 to August 1995, *Tech. Rep. Misc. Pap. CERC-96-6*, U.S. Army Eng. Waterways Exp. Stn., Vicksburg, Miss., 1996.

Longuet-Higgins, M. S., and R. W. Stewart, Radiation stress and mass transport in gravity waves, with application to "surf-beats," *J. Fluid Mech.*, *13*, 481–504, 1962.

Longuet-Higgins, M. S., and R. W. Stewart, Radiation stresses in water waves; A physical discussion, with applications, *Deep Sea Res. Oceanogr. Abstr.*, *11*, 529–562, 1964.

Miller, H. C., W. A. Birkemeier, and A. E. Dewall, Effects of CERC research pier on nearshore processes, in *Proceedings on Coastal Structures '83*, edited by J. R. Weggel, pp. 769–784, Am. Soc. of Civ. Eng., New York, 1983.

Nielsen, P., Wave setup: A field study, *J. Geophys. Res.*, *93*, 15,643–15,652, 1988.

Pawka, S. S., Island shadows in wave directional spectra, *J. Geophys. Res.*, *88*, 2579–2591, 1983.

Raubenheimer, B., R. T. Guza, and S. Elgar, Wave transformation across the inner surf zone, *J. Geophys. Res.*, *101*, 25,589–25,598, 1996.

Rennie, S. E., J. L. Largier, and S. J. Lentz, Observations of a pulsed buoyancy current downstream of Chesapeake Bay, *J. Geophys. Res.*, *104*, 18,227–18,240, 1999.

Sallenger, A. H., and R. A. Holman, Wave energy saturation on a natural beach of variable slope, *J. Geophys. Res.*, *90*, 11,939–11,944, 1985.

Schäffer, H. A., P. A. Madsen, and R. Diegaard, A Boussinesq model for waves breaking in shallow water, *Coastal Eng.*, *20*, 185–202, 1993.

Svendsen, I. A., Mass flux and undertow in a surf zone, *Coastal Eng.*, *8*, 347–365, 1984.

Wearn, R. B., Jr., and N. G. Larson, Measurements of the sensitivities and drift of Digiquartz pressure sensors, *Deep Sea Res.*, *Part A*, *29*, 111–134, 1982.

─────────────

S. Lentz and B. Raubenheimer, Department of Physical Oceanography, Woods Hole Oceanographic Institution, Woods Hole, MA 02543. (slentz@whoi.edu)